

# Different provenance of separate loess sites in Yangtze River Basin and its paleoenvironmental implications

ZHANG Zhi<sup>1,2</sup>  <https://orcid.org/0000-0002-3883-9085>; e-mail: 360435931@qq.com

JIA Yu-lian<sup>1\*</sup>  <https://orcid.org/0000-0002-5165-4130>;  e-mail: northforest@sohu.com

\* Corresponding author

<sup>1</sup> School of Geography and Environment, Key Laboratory of Poyang Lake Wetland and Watershed Research, Ministry of Education, Jiangxi Normal University, Nanchang 330022, China

<sup>2</sup> College of Chemistry and Chemical Engineering, Jiangxi Normal University, Nanchang 330022, China

**Citation:** Zhang Z, Jia YL (2019) Different provenance of separate loess sites in Yangtze River Basin and its paleoenvironmental implications. Journal of Mountain Science 16(7). <https://doi.org/10.1007/s11629-018-5278-6>

© Science Press, Institute of Mountain Hazards and Environment, CAS and Springer-Verlag GmbH Germany, part of Springer Nature 2019

**Abstract:** The dust deposits in the Yangtze River Basin (YRB) have been widely distributed along the Yangtze River valley. Previous studies mainly concentrated in its provenance of each loess site, however, the differences in provenance of loess among different sites in this area have rarely been studied. Here, the geochemical characteristics of the <20 µm fraction in the loess in separate Jiujiang, Xuancheng and Nanjing sites were analyzed. The result shows that the loess in Jiujiang and Nanjing sites, near Yangtze River riverway, share similar geochemical characteristics that may commonly derived from the detrital materials of Yangtze River. However, both sites have significantly different elemental compositions compared with Xuancheng site, which is ~60 km away from the Yangtze River riverway. These sites share different geochemical characteristics with Eastern Qinling Mountains and Xifeng section on the Chinese Loess Plateau, North China. Combining the distribution of the aeolian sand hills and the loess in this area published by previous studies, we suggest that the exposed river valley floodplain caused by weak summer monsoon provided abundant materials to form local dust cells controlled by strong winter monsoon during the glacial periods. Therefore, those local loess deposits should be identified as the “valley-sourced loess”.

**Received:** 31-Oct-2018

**Revised:** 14-Apr-2019

**Accepted:** 05-May-2019

These reveal the inherent connection between the monsoon system and the loess deposits in Yangtze River Basin.

**Keywords:** Yangtze River Basin; Geochemistry; Loess provenance; Valley-sourced loess; Loess Plateau

## Introduction

The loess deposits in the Yangtze River Basin (YRB), aka “Xiashu loess”, are an important component of aeolian deposits outside the Chinese Loess Plateau (CLP), which are one of the best terrestrial archives to documents East Asian monsoon and regional paleoenvironments changes (e.g. Liu 1985; An et al. 2001; Ding et al. 1995; Meng et al. 2015; Meng et al. 2018; Sun et al. 2019). They are widely distributed in river terraces of YRB and its adjacent hills and foothills (Yang et al. 1991), which are mainly located at Jiujiang site in the south, Xuancheng site in the middle and Nanjing site in the north (Figure 1). They are uniform and unstratified in texture with silt as main particle composition. Its minerals are dominated by quartz and feldspar and comprise some heavy minerals such as magnetite, pyroxene and zircon (Xu et al.

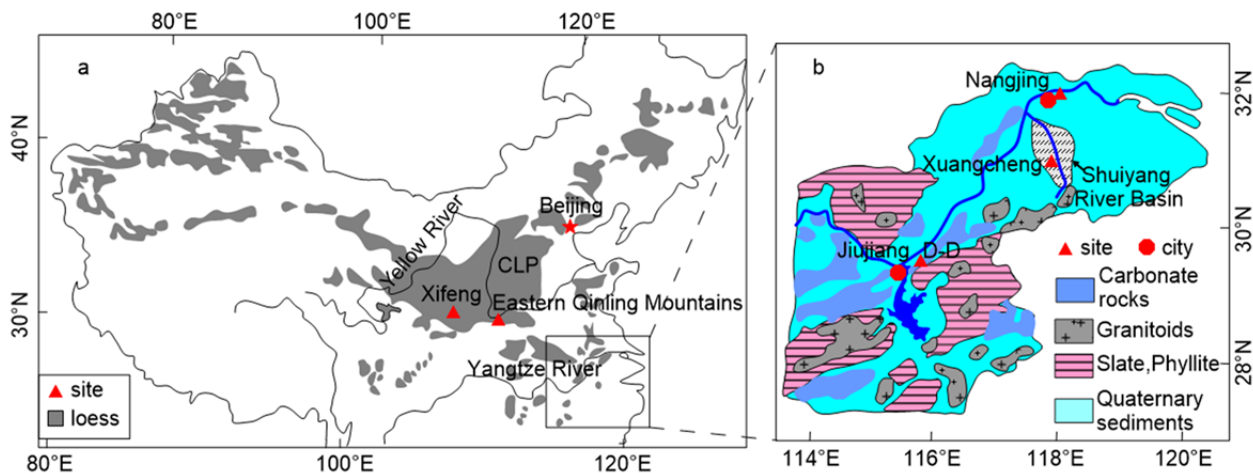


**Figure 1** Distribution of Chinese loess (a), rock types (b) in Yangtze River Basin and the locations of loess sections. Loess distribution based on Liu (1985); rock types distribution from Yang et al. (2009).

1991; Li et al. 1993; Li et al. 2009). YRB Xiashu loess is a ubiquitous surficial geologic deposit over much of the YRB and form the parent material for some of most productive soils for agriculture.

Recent studies showed that the formation of Xiashu loess is the direct indicator of regional environment change during late Quaternary (Li et al. 2017; Wang et al. 2018). The uncertainty about source of Xiashu loess limits our understanding of the environment change in YRB. The source of Xiashu loess in YRB has brought about widespread attention (e.g. Yang et al. 1991; Hu & Gong. 1999; Zheng et al. 1995; Xiong et al. 1999; Chen et al. 2008; Hao et al. 2010; Jia et al. 2012; Hu et al. 2013; Liu et al. 2014; Li et al. 2017). The Sr-Nb isotopic values and elements compositions of loess in the middle reaches of Yangtze River can be distinguished from those from loess in CLP (Qiao et al. 2011; Hong et al. 2013). In contrast, significant similarities in above date, exist between Xiashu loess in the lower reaches of Yangtze River and loess deposits of CLP (Chen & Li. 2011; Qian et al. 2018). Moreover, U-Pb ages of zircon grains extracted from the Xiashu river from lower reaches Yangtze River indicating the dominance proximal source of dust (Liu et al. 2014; Qian et al. 2018). Therefore, the constraint of provenance of Xiashu loess in YRB is very necessary. In this paper, the geochemical characteristics of loess from Jiujiang and Nanjing sites together with Xuancheng loess published by Hao et al. (2010) are studied. The differences of loess materials are discussed using the geochemical characteristics of loess from three

sites and implicating for local paleoclimatic changes in finally.

## 1 Sampling and Analytical Methods

The samples were collected from the northeastern location of Poyang Lake in Jiangxi Province near Jiujiang and Nanjing areas. Three profiles (Figure 1b) were sampled and named D-D-01 ( $29^{\circ}50'12''N$ ,  $116^{\circ}24'49''E$ ), D-D-02 ( $29^{\circ}49'47.6''N$ ,  $116^{\circ}25'1.5''E$ ), D-D-03 ( $29^{\circ}46'52.4''N$ ,  $116^{\circ}24'59.2''E$ ), respectively. Three loess profiles, deposited during last glacial period (Lai et al. 2010; Jia et al. 2012), are located on the south of aeolian dunes in Hukou and Pengze. The D-D-01 section deposited a total thickness of ~14m, and was exposed due to a local construction project. It consists of aeolian sand layer (2 m) in the top and loess layer (~12 m) in the bottom. Five loess samples were collected at depths of 2.5, 3.5, 4.5, 6.5 and 7.5 m. The D-D-02 section is ~8m in thickness with clearly vertical joints. Four loess samples in D-D-02 section were obtained at depths of 1.2, 4.2, 6.2 and 7.2 m in total~8m thickness with clearly vertical joints. The D-D-03 section is ~4 km away from the D-D-02, with a thickness of ~8 m and five loess samples were chosen at depths of 0.6, 2.6, 4.6, 6.6 and 7.6 m.

The Nanjing loess was collected from Yanziji section with a thickness of ~8m (Figure 1b) located in the south of Yangtze River ( $32^{\circ}08'46''N$ ,  $118^{\circ}48'48''E$ ). This section consists of loess (2.8 m), paleosol (2.4 m) and loess (2.6 m) from top to

**Table 1** Mean concentrations (wt %) of major elements in the <20 µm fraction of loess from Jiujiang, Nanjing, Xuancheng, Xifeng and Eastern Qinling mountains. Xuancheng and Xifeng are from Hao et al. (2010); Eastern Qinling Mountains are from Li et al. (2016).

Oxide (%)	Jiujiang loess				Nanjing loess	Xuancheng loess	Xifeng loess	Eastern Qinling mountains
	D-D-01 n=5	D-D-02 n=4	D-D-03 n=5	Average	n=10	n=5	n=5	n=23
SiO <sub>2</sub>	64.20	62.36	67.06	64.54	60.28	70.52	63.07	69.72
Al <sub>2</sub> O <sub>3</sub>	13.89	16.02	13.76	14.56	15.90	17.84	18.38	15.90
Fe <sub>2</sub> O <sub>3</sub>	4.32	5.46	4.26	4.68	5.47	6.76	7.86	5.60
MgO	1.40	1.20	1.07	1.22	1.42	0.84	3.53	1.97
CaO	1.04	0.64	0.70	0.79	1.09	0.12	1.27	0.49
K <sub>2</sub> O	2.52	2.38	2.38	2.43	2.63	2.24	3.48	3.07
Na <sub>2</sub> O	1.37	0.81	0.96	1.05	0.85	0.26	1.26	1.96
TiO <sub>2</sub>	0.79	0.89	0.86	0.85	0.85	1.23	0.84	1.04
P <sub>2</sub> O <sub>5</sub>	0.24	0.08	0.07	0.13	0.16	0.08	0.17	0.15
MnO	0.08	0.02	0.01	0.04	0.10	0.13	0.14	0.10
CIA	66.92	75.82	71.72	71.49	70.07	76.47	67.31	62.04

bottom. A total of ten samples were collected at the upper layer with ~0.5 m intervals. Previous geochronological works have revealed that the upper layer (5.2m) deposited during the last glacial period (Lai et al. 2001; Yi et al. 2018).

Above selected loess samples were measured for major and trace elements. The major elements were measured using the German S4PINOER X ray fluorescence spectrometer at the Physical and Chemical Tests Center of Jiangxi Normal University. Trace element concentrations were measured using Inductively Coupled Plasma Mass Spectrometry (ICP-MS) in the Institute of Tibetan Plateau research, Chinese Academy of Sciences. In order to examine effect of the long-term components, all samples were tested the <20 µm fraction, as only this fraction of dust can be transported in long-term suspension over long distance (Tsoar et al. 1987). Moreover, the <20 µm fraction represents the major component of samples (Jia et al. 2012; Hu et al. 2013). This fraction was pipetted from suspension based on Stoke's Law.

## 2 Results

### 2.1 Characteristics of Major Elements

The results of major elements show that the relative errors of Na and Ca between the tested and parallel samples are 5.2% and 1.1%, respectively, while the results of Fe, K, Si, Al and Mg are less than 1%. Table 1 shows the major elements in <20

µm fraction in the Jiujiang, Nanjing, Xuancheng, Xifeng and Eastern Qinling Mountains with domination of SiO<sub>2</sub>, Al<sub>2</sub>O<sub>3</sub> and Fe<sub>2</sub>O<sub>3</sub>. The average content of SiO<sub>2</sub>, Al<sub>2</sub>O<sub>3</sub> and Fe<sub>2</sub>O<sub>3</sub> in Jiujiang loess is about 64.5%, 14.6% and 4.7%, respectively. The sum of those three oxides is 83.8% of the total elements. The contents of those three elements in Nanjing loess are 60.3%, 15.9% and 5.5%, respectively, accounting for 81.7% of the total elements. It is similar to Jiujiang loess. While the proportion of that in Xuancheng, Xifeng and East Qinling Mountains loess is 95.1%, 89.3% and 91.2%, respectively, showing a certain difference from Jiujiang and Nanjing. Other elements such as MgO, CaO, K<sub>2</sub>O, Na<sub>2</sub>O, TiO<sub>2</sub> and MnO also show the same characteristics between Jiujiang and Nanjing loess. For evaluating influence of chemical weathering, the chemical index of alteration (CIA, CIA=Al<sub>2</sub>O<sub>3</sub>/(Al<sub>2</sub>O<sub>3</sub>+CaO<sup>\*</sup>+Na<sub>2</sub>O+K<sub>2</sub>O)×100, in molecular proportions, where CaO<sup>\*</sup> is the amount of CaO in silicate minerals) values has been used. The CIA values in Jiujiang and Nanjing loess are very close, with average of 71.5 (n=14) and 70.1 (n=10), respectively. It indicates that both sites experienced moderate intensity chemical weathering. The CIA of Xifeng and East Qinling Mountains are 67.3 and 62.0, respectively, reflecting weak chemical weathering intensity. The Xuancheng loess has experienced strongest weathering indicated by the highest CIA value (mean 76.5).

Compared with the upper continental crust (UCC) (Figure 2), the distribution of major elements in the YRB loess showed the following

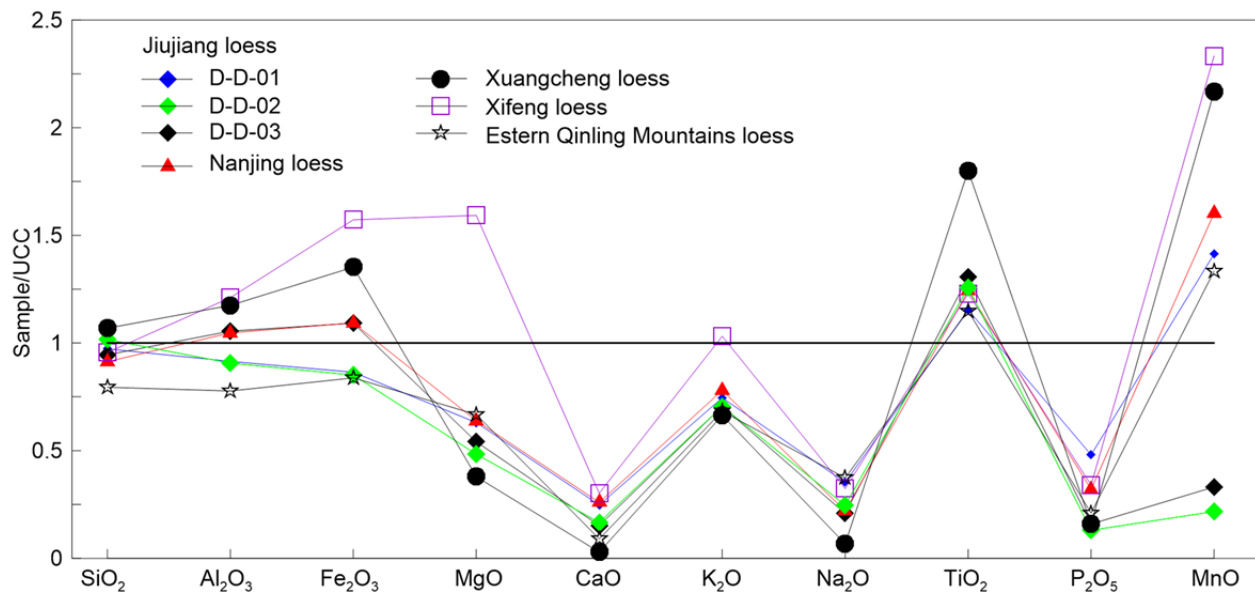


**Figure 2** The upper continental crust (UCC)-normalized curve of major elements in the  $<20\text{ }\mu\text{m}$  fraction of loess from Jiujinag, Nanjing, Xuancheng, Xifeng and Eastern Qinling mountains. UCC are from Taylor and McLennan(1985); Xuancheng and Xifeng are from Hao et al. (2010); Eastern Qinling Mountains are from Li et al. (2016).

characteristics: 1) the distribution patterns of  $\text{Fe}_2\text{O}_3$  and  $\text{MnO}$  are quite different, and the other elements have similar changes; 2) the distribution patterns of some elements, such as Fe, Mg and K in Xifeng loess, obviously different from those in other loess regions. The  $\text{TiO}_2$  of Xuancheng loess differs greatly from that of other YRB loess; 3) compared with UCC,  $\text{MgO}$ ,  $\text{CaO}$ ,  $\text{K}_2\text{O}$ ,  $\text{Na}_2\text{O}$  and  $\text{P}_2\text{O}_5$  are relative loss and  $\text{TiO}_2$  is relatively enriched. The major elements Ti and Al have extremely low

solubility, and are very stable during the postdeposition (Broecker & Peng 1982; Sugitani et al. 1996). The  $\text{TiO}_2$  content of different rocks is differentiated, but the content of  $\text{Al}_2\text{O}_3$  is relatively constant. Therefore, the  $\text{TiO}_2/\text{Al}_2\text{O}_3$  ratio has been often used to distinguish the source of dust (Sheldon & Tabor 2009; Hao et al. 2010). The  $\text{TiO}_2/\text{Al}_2\text{O}_3$  value of the  $<20\text{ }\mu\text{m}$  fraction particles in Jiujiang loess is near and slightly higher than that of Nanjing and Xifeng loess, but it is obviously lower than that of East Qinling Mountains and Xuancheng loess (0.053-0.065, with an average of 0.059) (Figure 3).

The  $\text{K}_2\text{O}/\text{Al}_2\text{O}_3$  ratio can be used as a tracer of provenance (Cox et al. 1995; Muhs et al. 2016) when the sediments experienced weak chemical weathering. The  $\text{K}_2\text{O}/\text{Al}_2\text{O}_3$  value is close between Nanjing and Jiujiang loess (from 0.140 to 0.193, with an average of 0.169). It is lower than that of East Qinling Mountains and Xifeng loess, and higher than that of Xuancheng loess.  $\text{K}_2\text{O}/\text{Al}_2\text{O}_3$  ratio of Xuancheng loess is low as it has experienced a relatively strong chemical weathering. In the  $\text{K}_2\text{O}/\text{Al}_2\text{O}_3$  vs.  $\text{TiO}_2/\text{Al}_2\text{O}_3$  scatter plot (Figure 3), the Jiujiang, Nanjing and East Qinling Mountains loess is adjacent. They are far away from the loess of Xuancheng and Xifeng, which are not overlapping each other, suggesting significant differences between in the sources.

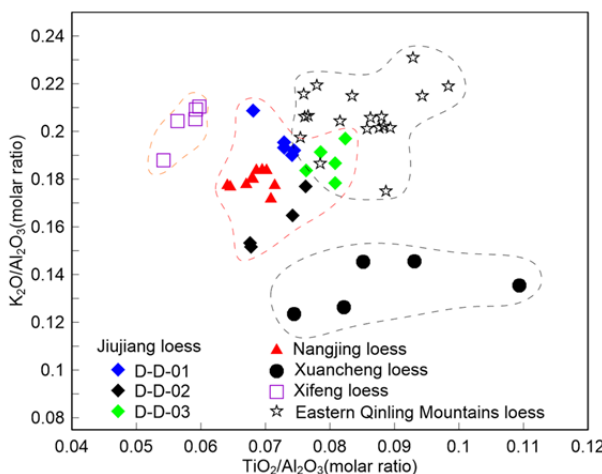


**Figure 3** Scatter-chart of major elements for  $<20\text{ }\mu\text{m}$  fraction of loess from Jiujinag, Nanjing, Xuancheng, Xifeng and Eastern Qinling mountains. Xuancheng and Xifeng are from Hao et al. (2010); Eastern Qinling Mountains are from Li et al. (2016).

**Table 2** Mean concentrations (ppm) of trace elements in the <20 $\mu\text{m}$  fraction of loess from Jiujiang, Nanjing, Xuancheng, Xifeng and East Qinling mountains. Xuancheng and Xifeng are from [Hao et al. \(2010\)](#); Eastern Qinling Mountains are from [Li et al. \(2016\)](#).

Elements (ppm)	Jiujiang loess			Nanjing loess	Xuancheng loess	Xifeng loess	Eastern Qinling mountains
	D-D-01 <i>n</i> =5	D-D-02 <i>n</i> =4	D-D-03 <i>n</i> =5	<i>n</i> =10	<i>n</i> =5	<i>n</i> =5	<i>n</i> =23
Li	21.29	32.71	31.53	31.30	63.60	54.92	49.09
Be	1.45	1.19	1.23	1.28	2.59	2.64	2.40
Sc	9.55	9.81	9.90	9.46	13.90	16.80	14.56
V	71.05	76.37	77.77	73.40	121.00	117.04	113.38
Co	1.22	0.66	0.78	1.43	17.20	20.73	17.72
Ga	12.99	13.55	13.95	14.25	21.40	21.31	20.70
Rb	107.30	106.01	108.65	111.54	119.000	124.54	128.29
Sr	126.65	93.35	91.08	104.07	52.70	113.13	102.13
Y	25.54	26.54	27.29	25.56	29.5	22.62	18.56
Zr	452.28	449.40	438.22	432.43	238.00	151.24	161.13
Nb	19.27	21.35	21.17	17.80	25.00	16.26	21.42
Ba	510.63	466.53	490.15	434.17	489.00	577.68	530.43
La	26.31	23.58	23.07	31.12	44.40	33.44	35.79
Ce	53.19	47.47	46.05	62.00	89.30	66.85	69.97
Pr	5.74	5.12	4.99	7.01	9.97	7.38	7.73
Nd	20.99	18.68	18.17	25.35	36.00	28.02	28.26
Sm	3.76	3.34	3.32	4.62	6.50	5.27	5.03
Eu	0.76	0.68	0.69	0.88	1.20	1.02	0.96
Gd	3.58	3.29	3.36	4.17	5.23	4.37	3.85
Tb	0.61	0.59	0.61	0.64	0.88	0.75	0.71
Dy	3.94	3.97	4.12	4.14	5.16	4.42	3.63
Ho	0.85	0.88	0.91	0.87	1.01	0.89	0.71
Er	2.63	2.77	2.82	2.74	2.84	2.52	2.16
Tm	0.40	0.43	0.43	0.41	0.44	0.39	0.37
Yb	2.79	3.00	2.99	2.75	2.90	2.51	2.44
Lu	0.43	0.45	0.45	0.42	0.44	0.38	0.37
Hf	10.81	10.64	10.43	9.39	6.53	4.69	3.99
Ta	1.55	1.52	1.54	1.16	1.87	1.25	1.54
Tl	0.46	0.47	0.48	0.47	0.66	0.75	0.78
Pb	7.75	6.20	5.79	5.95	29.30	35.70	21.26
Bi	0.05	0.03	0.025	0.05	0.36	0.50	0.32
Th	9.16	7.86	7.84	8.69	15.80	13.88	11.29
U	3.01	3.01	3.09	2.65	3.81	2.97	2.44

## 2.2 Characteristics of trace elements

In the trace elements test, the relative error of Be, V, Y and some heavy rare earth elements between the test samples and the parallel samples (Tb-Tm) ranges from 11% to 16%, and that of the other elements is between 0%~8%.

[Table 2](#) shows the trace element (including REE) contents of the <20  $\mu\text{m}$  fraction in the loess areas of Jiujiang, Nanjing, Xuancheng, Xifeng and East Qinling Mountains. The normalized distribution patterns of UCC are shown in [Figure 4](#). The UCC-normalized trace element distribution patterns for the Jiujiang and Nanjing loess are rather uniform. These date showed concretely in: 1) Be, Sc, V, Co, Sr, Tl, Pb, Bi and other trace elements

were significant depletion, while Zr and Hf were significant enriched; 2) the distribution curve of light-REE (LREE) (La-Eu) was relatively flat, showing a slight depletion (Jiujiang loess) or basically consistent with UCC, and the distribution curve of heavy-REE(HREE) (Gd-Lu) steepened. While that of the loess in Xuancheng, Xifeng and East Qinling Mountains is quite different from those in Jiujiang and Nanjing, which showed that: 1) Li, Sc, V, Co, Ga, Rb, Nb, Ta, Pb and Th elements enriched, and the Li, Pb and Nb elements significantly enriched; 2) all REEs, except for slight losses of Ho and Er in East Qinling Mountains loess, enriched peaked at Xuancheng loess. The distribution patterns of loess elements in Jiujiang and Nanjing areas are similar, which are quite

different from those in Xifeng, East Qinling Mountains and Xuancheng sites.

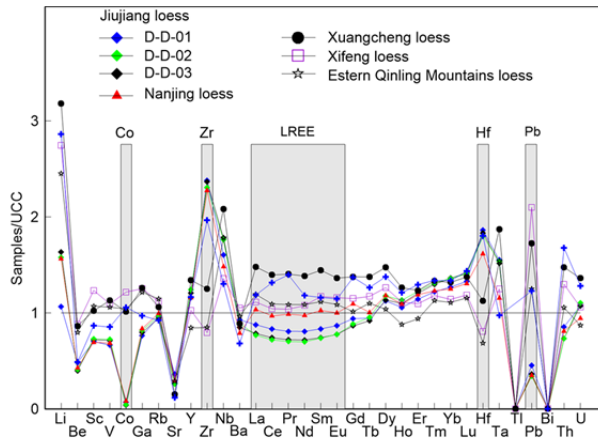


**Figure 4** The upper continental crust (UCC)-normalized curve of trace elements in the  $<20\mu\text{m}$  fraction of loess from Juijinag, Nanjing, Xuancheng, Xifeng and Eastern Qinling mountains. UCC are from Taylor and McLennan (1985); Xuancheng and Xifeng are from Hao et al. (2010); Eastern Qinling Mountains are from Li et al. (2016).

In order to further explain the geochemical characteristics of loess that mentioned, the following elements of stable elements and their ratios are selected to reveal the similarities and differences of the provenance of loess.

The distribution characteristics of some stable REEs in the clastic sediments inherit and retain the characteristics of its source area (Taylor & McLennan 1985), so they are potential as indicators of provenance tracing. This method has been applied in the provenance study of loess in the YRB (Chen et al. 2008; Hao et al. 2010; Qiao et al. 2011). For example, the  $\text{La}_N/\text{Yb}_N$  value (chondrite-normalized data) can represent the fractionation of LREE and HREE (Hao et al. 2010), and the  $\text{Eu}/\text{Eu}^*$  value (where  $\text{Eu}$  is  $\text{Eu}_N$ , and  $\text{Eu}^*$  is  $(\text{Sm}_N^*/\text{Gd}_N)^{0.5}$ ) mainly reflects the geochemical information of the source rocks in the source area (Gallet et al. 1996).

Figure 5 indicates that the  $\text{La}_N/\text{Yb}_N$  ratios (from 4.589 to 7.186, with an average of 5.665) and  $\text{Gd}_N/\text{Yb}_N$  (from 0.848 to 0.1087, with an average of 0.950) are the lowest in Juijiang loess, followed by Nanjing loess, and others are the highest. In the  $\text{La}_N/\text{Yb}_N$  vs.  $\text{Eu}/\text{Eu}^*$  and  $\text{La}_N/\text{Sm}_N$  vs.  $\text{Gd}_N/\text{Yb}_N$  scatter diagram, the loess of Juijiang, Nanjing, Xuancheng, Xifeng and East Qinling Mountains each occupies a certain space position. The Xuancheng, Xifeng and East Qinling Mountains

loess have some overlaps and Juijiang and Nanjing loess are the closest.

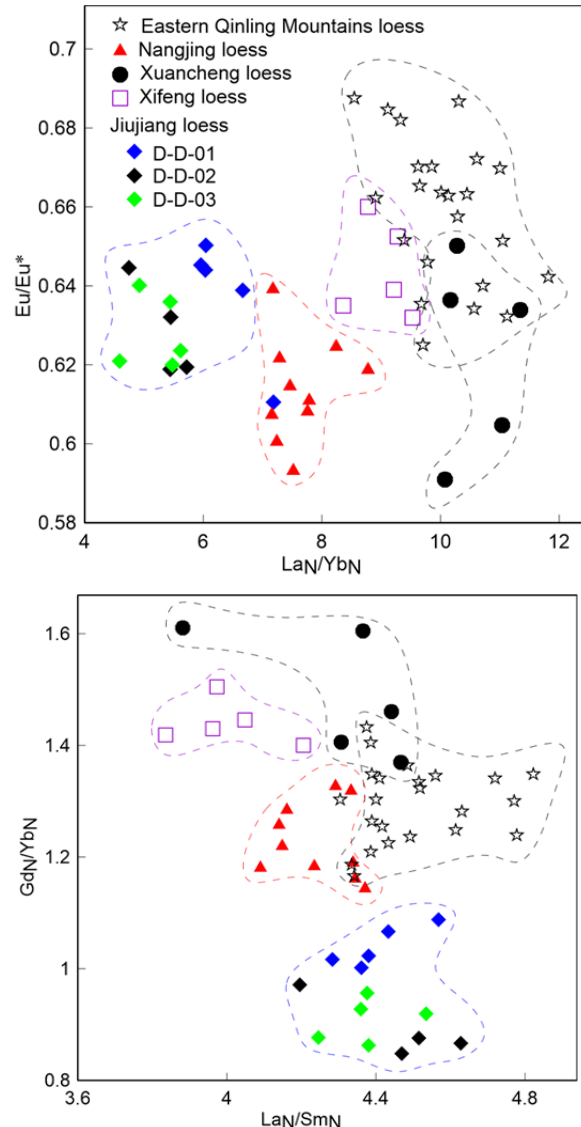


**Figure 5** REE scatter chart of  $<20\mu\text{m}$  fraction of loess from Juijinag, Nanjing, Xuancheng, Xifeng and Eastern Qinling mountains. Xuancheng and Xifeng are from Hao et al. (2010); Eastern Qinling Mountains are from Li et al. (2016).

The high field strength elements (mainly including Nb, Ta, Zr, Hf, Ti and Th) and Al elements have high particle potential energy. Their compounds are extremely difficult to dissolve in water. They are inert components in the epigenetic process and are not easily depletion. Therefore, these elements have the ability to inherit the geochemical characteristics of source rocks and have strong indication of provenance. For example, Zr and Hf elements can be completely

homogeneous and representing the compositions for zircons in the deposits (Bhatia & Crook., 1986; Barth et al. 2000; Samuel et al. 2005). Therefore, the ratios of those elements (e.g., La/Nb, Th/Nb, Zr/Al, Y/Al, etc.) are commonly used in elemental geochemical tracing studies (Sun, 2002; Hao et al. 2010; Muhs. 2018). Compared Jiujiang and Nanjing loess with the other three sites, the ratios of Th/Nb (from 0.313 to 0.549, with an average of 0.393), La/Nb (from 1.202 to 1.303, with an average of 1.248) and Y/Al (from 1.659 to 2.374, with an average of 2.036) are lower, while the ratios of Zr/Nb (from 15.533 to 29.783, with an average of 20.710), Hf/Nb (from 0.342 to 0.690, with an average of 0.478), Zr/Al (from 2.484 to 3.613, with an average of 3.004), Zr/Ti (from 4.479 to 6.223, with an average of 5.324), Al/Nb (from 6044 to 8855, with an average of 7517) and Ti/Nb (from 262 to 326, with an average of 299) are higher (Figure 6). The above elemental ratios of loess in Jiujiang and Nanjing are concentrated and even covered with each other, which are quite different from Xuancheng, Xifeng and Eastern Qinling Mountains loess. The latter are far away from each other and occasionally overlap each other on the scatter diagram, and mainly occur in

REEs.

### 3 Discussion

#### 3.1 Provenance of loess in the YRB and the local aeolian sand-dust depositional cells

The study of provenance of loess is a very complicated issue and involves a series of variables that difficult to accurately determine, such as complex source rock, wind sorting, pedogenesis etc. (Marx 2005; Chen & Li 2011; Muhs 2013). Therefore, multi-proxy analysis methods should be used to trace the provenance of aeolian loess (Qian et al. 2018). Geochemical methods are one of the most widely used approaches in loess provenance tracing study. For example, high field-strength elements and REE in clastic sediments still maintain the geochemical characteristics of their source after postdeposition, and then they are well tracer elements (Talyor & McLennan 1985) verified by recent studies (Cox et al. 1989; Sun 2002; Guan et al. 2008; Muhs et al. 2008; Hao et al. 2010; Muhs et al. 2016, 2018). Traditionally, the plots described by major elements and trace elements

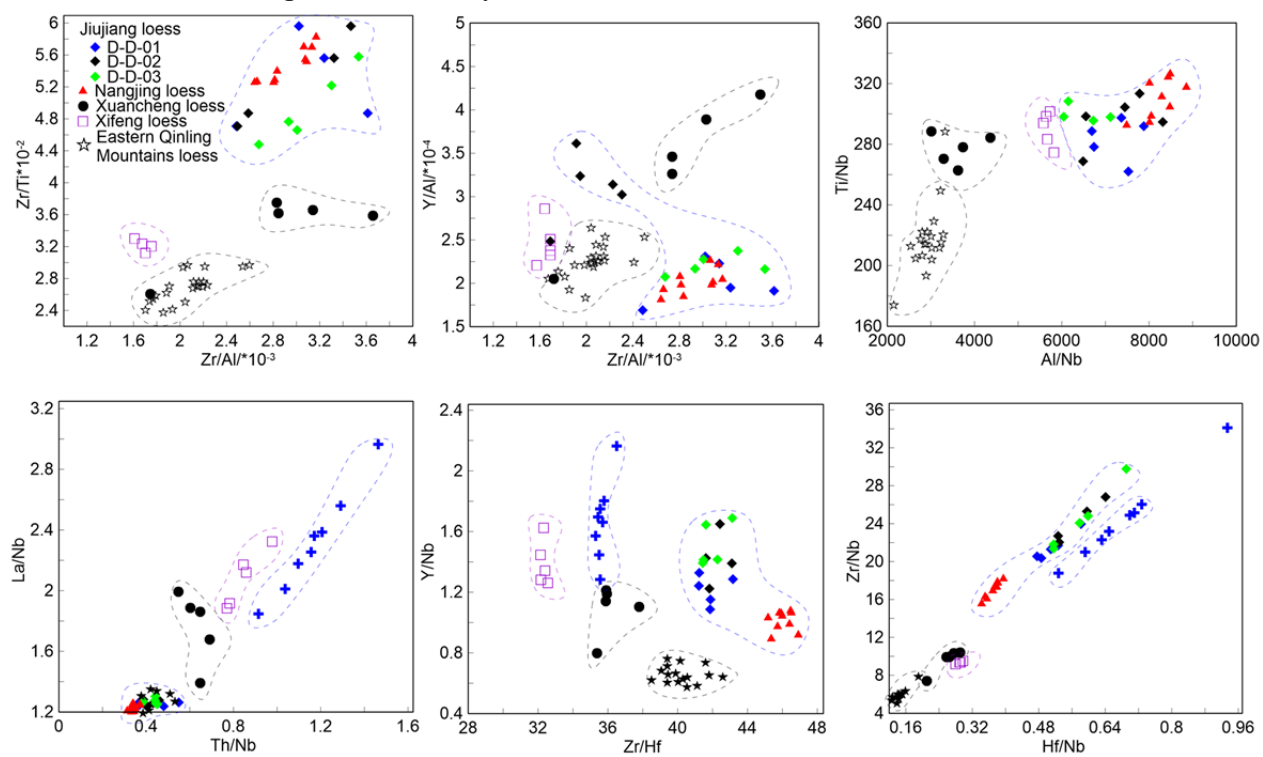


**Figure 6** Scatter charts of high field-strength element in  $<20 \mu\text{m}$  fraction of loess from Jiujiang, Nanjing, Xuancheng, Xifeng and Eastern Qinling mountains. Xuancheng and Xifeng are from Hao et al. (2010); Eastern Qinling Mountains are from Li et al. (2016).

**Table 3** The value of significance (sig) between loess sites.

Element ratios	JJ vs. NJ	JJ vs. XF	JJ vs. XC	JJ vs. EQL	NJ vs. XF	NJ vs. XC	NJ vs. EQL	XF vs. XC	XF vs. EQL	XC vs. EQL
$Gd_N/Yb_N$	0.000	0.000	0.000	0.000	0.000	0.003	0.055	0.374	0.000	0.010
$La_N/Sm_N$	0.002	0.000	0.174	0.272	0.002	0.597	0.000	0.046	0.000	0.165
$Eu/Eu^*$	0.003	0.088	0.330	0.000	0.001	0.465	0.000	0.138	0.020	0.017
$La_N/Yb_N$	0.000	0.000	0.000	0.000	0.000	0.000	0.000	0.001	0.014	0.046
$K_2O/Al_2O_3$	0.424	0.018	0.000	0.010	0.000	0.000	0.004	0.000	0.480	0.000
$TiO_2/Al_2O_3$	0.001	0.000	0.075	0.007	0.000	0.024	0.007	0.005	0.003	0.554
$Y/Al$	0.679	0.004	0.022	0.052	0.001	0.020	0.027	0.047	0.098	0.028
$Zr/Al$	0.292	0.000	0.270	0.000	0.000	0.519	0.000	0.006	0.000	0.100
$Y/Nb$	0.000	0.347	0.001	0.000	0.000	0.966	0.000	0.013	0.002	0.089
$Zr/Hf$	0.000	0.000	0.000	0.001	0.000	0.000	0.000	0.000	0.000	0.000
$Zr/Nb$	0.000	0.000	0.000	0.000	0.000	0.000	0.000	0.642	0.003	0.014
$Hf/Nb$	0.000	0.000	0.000	0.000	0.000	0.000	0.000	0.136	0.000	0.002
$Zr/Ti$	0.121	0.000	0.000	0.000	0.000	0.000	0.000	0.284	0.000	0.021
$Zr/Al$	0.292	0.000	0.181	0.000	0.000	0.365	0.000	0.006	0.000	0.101
$Al/Nb$	0.000	0.000	0.000	0.000	0.000	0.000	0.000	0.000	0.000	0.037
$Ti/Nb$	0.004	0.005	0.000	0.000	0.000	0.000	0.000	0.092	0.000	0.000
$La/Nb$	0.000	0.001	0.009	0.000	0.000	0.007	0.000	0.044	0.010	0.755
$Th/Nb$	0.000	0.000	0.000	0.001	0.000	0.000	0.000	0.001	0.000	0.000

**Notes:** JJ=Jiujiang loess; NJ=Nanjing loess; XC=Xuancheng loess; XF=Xifeng loess; EQL= Eastern Qinling mountains; Sig=2-tailed.

are often used in provenance identification (Muhs & Bettis 2000; Sun 2002; Hao et al. 2010; Chen & Li 2011; Muhs et al. 2018). In this study, the independent t-test was also employed to confirm the reliability of elemental ratios. The values of significance (sig) were obtained by SPSS 20.0. Table 3 lists the value of significance of each loess site in 90% significance level. In this table, the sig<0.05 indicates that the values of element ratios between loess sites are marked difference, and vice versa. After cross-checked the location of the element ratios of each site on the plots with the t-tests results, we found that if there was a significant difference between two element ratios (sig<0.05), the scatters of all element ratios would fall in different areas on the plot; opposite to occurs during sig>0.05. Therefore, the difference of geochemistry of loess in all sites can be reflected by the bivariate plots effectively. Through the comparison of the geochemical date of loess from Jiujian, Xuancheng, Nanjing, Xifeng and Eastern Qinling, we suggest that the major and trace elements characteristic of Jiujian and Nanjing Xiashu loess are similar. However, they are different from loess in the Xuancheng, Xifeng and Eastern Qinling sites.

The age spectra of detrital zircon have the advantage as an accurate source tracer due to the resistance of zircon to weathering. Recently, a large dataset of zircon ages has been established for the

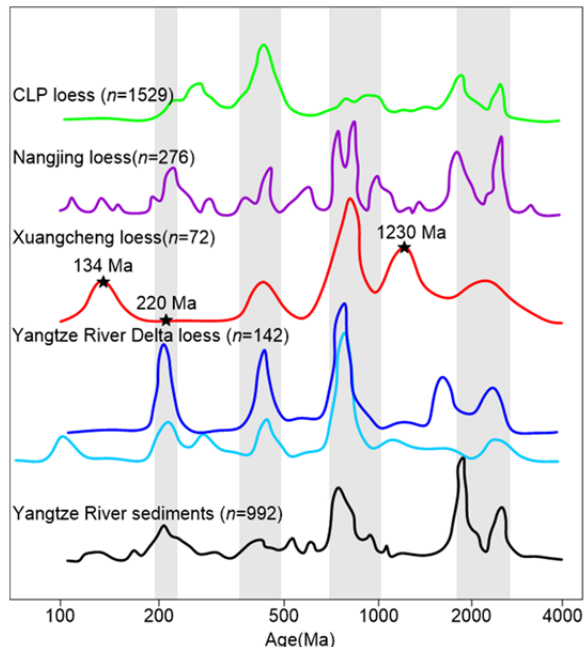


**Figure 7** Density plots of zircon age distributions for: the Xuangcheng loess; the Nangjing loess; the Yangtze River Delta loess; the Chinese Loess Plateau loess; and the Yangtze River sediments. All data are from Qian et al. (2018).

Xiashu loess on the lower reaches of Yangtze River (Liu et al. 2014; Qian et al. 2018). Results showed that the Xiashu loess and the sediments of the YRB share considerable similarity in their zircon U-Pb age spectra. By

contrast, significant differences exist between the Xiashu loess and loess of CLP (Figure 7). On the other hand, the age spectra of zircon in Xiashu loess are not completely consistent in the interior of three sites. The Xiashu loess from Nanjing and Yangtze River Delta shows great similarities in its zircon ages to the Yangtze River sediments, with the almost perfect matching of major peaks. In contrast, the high ~134 Ma and ~1230 Ma peaks that characterize the Xiashu loess from Xuancheng were not observed in the Yangtze River sediments. The Yangtze River sediments have significant proportions of zircon with ages 220Ma peak; this is rarely found in the Xuancheng loess (Figure 7).

The dust materials originated from the northwestern arid areas are the main sources of the aeolian deposits in northern China (e.g., Sun 2002; Chen et al. 2007; Zhang et al. 2016; Meng et al. 2019) mainly transported by low-level Asian winter monsoon circulation (e.g., An 2000; Liu 1985). Blocked by high and huge mountains, the dust from northwestern arid areas of China can be hardly transported to YRB by winter monsoon (Sun et al. 2002). For instance, Mangshan loess in the middle reach of Yellow River was generated by proximal deposit of local dust transported by winter monsoon (Li et al. 2017; Yuan et al. 2018). Meanwhile, age spectra data of detrital zircon suggested that dust derived from Hetao and Ningxia plain is the main source of loess on the CLP (Nie et al. 2015). The widespread loess deposits in the Central Shandong Mountains also are originated from floodplain of low reach of Yellow River and/or exposed continental shelf of Bohai during glacial period (Peng et al. 2016; Li et al. 2017). Similar local scale dust deposits are commonly seen in Mississippi River Basin in North America and western Europe (Muhs & Bettis 2000; Muhs et al. 2003, 2018; García et al. 2011).

The foregoing discussion shows that the dust derived from upwind northwestern arid areas can't mass was move to YRB. The YRB is far away from the hinterland of Asian winter monsoon and has complex landforms, relatively closed environment and weak winter wind. Those conditions make the limited transport of and formed numerous local depositional cells. This is supported by the geochemical dissimilarities of loess from Jiujiang, Xuancheng and Nanjing area. For example, the

characteristic of geochemical elements of loess from Jiujiang and Nanjing are similar because of possible some provenance (e.g., Yangtze River floodplain) (Jia et al. 2012; Liu et al. 2014; Li et al. 2017; Wang et al. 2018). In contrast, the loess from Xuancheng is far away from Yangtze River riverway and is located in the closed Shuiyang river basin (Figure 1) (Yang et al. 1991). Therefore, the loess of Xuancheng may be derived from this local basin.

In the YRB, Qingshan (near Wuhan), Junshan (near lake Dongting), Jiujiang and Pengze on the southern bank of the Yangtze River, especially in the area surrounding Poyang lake, a series of sand hills are developed on the first or second terraces of the river and lake (Yang 1985; Zhuang et al. 2007; Jia et al. 2012). On the south side of those sand hills, there are different thicknesses of loess deposits in the direction of winter monsoon downwind. In the sand hill, those loess deposits and sand beds are often interbedded with each other (Figure 8) (Liu et al. 1997; Lai et al. 2010; Jia et al. 2012). Moreover, the thickness and grain size of loess decrease increasing distance compared with Yangtze River riverway (Li et al. 2006; Hu et al. 2013; Peng et al. 2014). Based on our tracing results, we suggest that the aeolian sand and loess should be the facies of the same local aeolian sand-dust depositional cell. The situations of eastern China may be similar to the middle reach of Yangtze River during glacial period. The facies of aeolian depositional units in this area include sand and Xiashu loess (Figure 8b) (Zhao et al. 1997).

### 3.2 Role of East Asian monsoon and rivers in loess formation over the YRB

Source and transport power are the preconditions in the formation of dust deposits (Muhs.2013; Guo 2017). The YRB are located in the East Asian monsoon hinterland, and the winter winds were strong during the glacial period. Some areas are affected by local topography, and the local wind is particularly strong (Yang 1991; Zhuang et al. 2007). Therefore, transport power is not a limited condition for the regional aeolian dust system, and the key point is the supply of material. In arid areas, the bare geomorphic environment, including glacial till, alluvial fan deposits, the dry river bed, and the dry lake beach, provides a

certain supply of dust material (Pye 1995). However, the YRB has not experienced periglacial environment since early Pleistocene (Yang 1985; Li et al. 2018). Even if the piedmont alluvial fan has a certain vegetation coverage (Liu et al. 1997) it is difficult to become the clastic supply area. Only the dry river valleys and lake beaches can provide a certain supply of detrital material. Therefore, the

Yangtze River and its first-class tributaries have played important roles in dust production.

The YRB is located in the East Asian monsoon hinterland. A large amount of detrital materials are brought into YRB by Yangtze River (including river valley and lake bed) in rainy season and/or interglacial period controlled by summer monsoon. These detrital materials are strongly exposed in

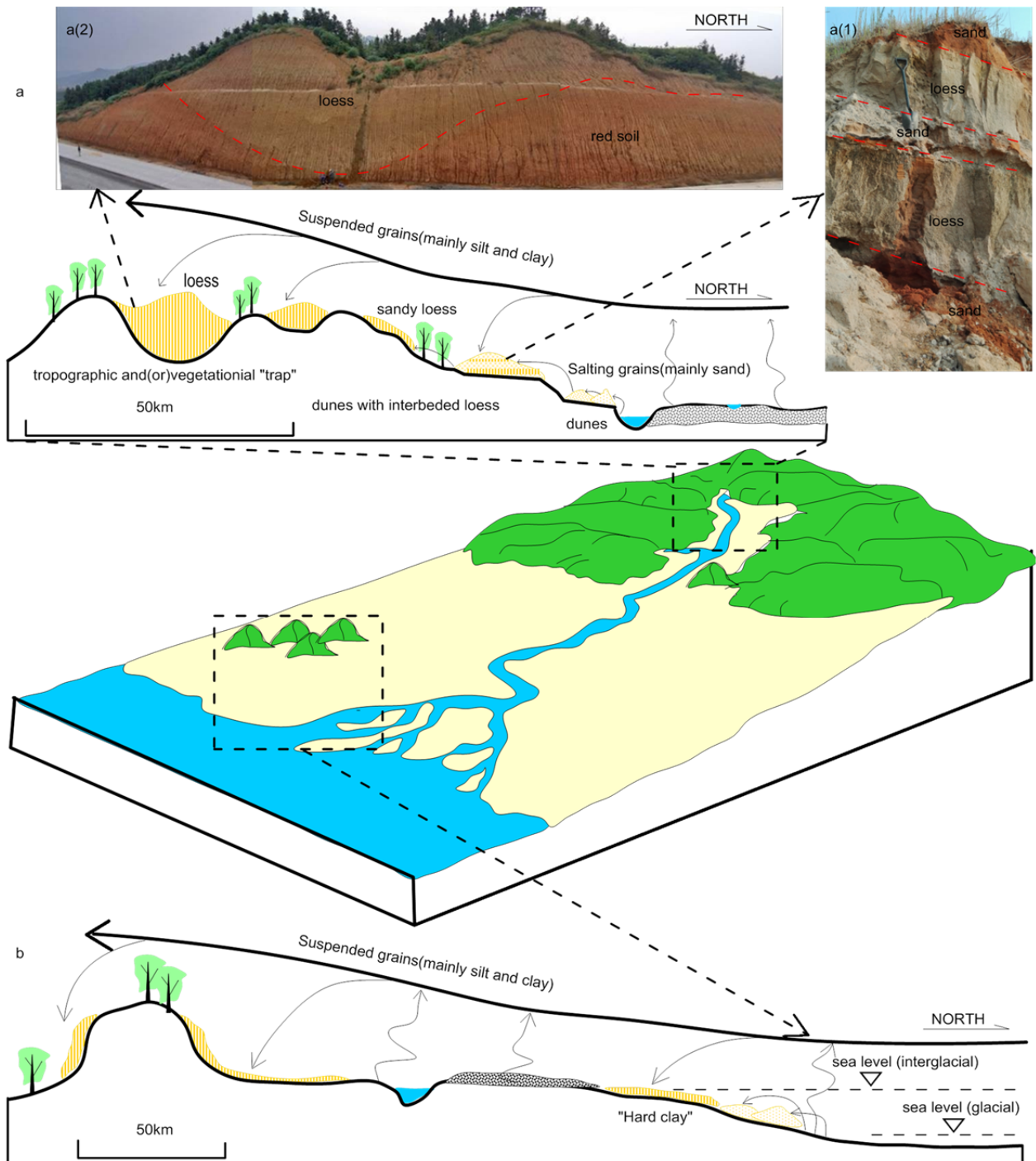


**Figure 8** Model of local aeolian depositional sand-dust cell and “fluvial” loess formation in the Yangtze River Basin.

arid periods and/or seasons, similar to winter and/or glacial epochs. Then the local aeolian cells were developed in the arid periods controlled by winter monsoon. Therefore, the East Asian monsoon plays an important role in aeolian deposits formation in this area. Since the large and medium-sized rivers and lakes play vital roles in dust supply, such loess can be called "valley-sourced loess" priority.

#### 4 Conclusion

The loess dust deposit in the monsoon region involves complicated geography, geomorphology, climate and environmental processes. Comparison and analysis of the geochemical characteristics of the  $<20\text{ }\mu\text{m}$  fraction in Jiujiang, Nanjing, Xuancheng, East Qinling Mountains and Xifeng, it is believed that the geochemical characteristics of the loess elements in Jiujiang and Nanjing are much similar but obviously different to those of Xuancheng, East Qinling Mountains and Loess Plateau Xifeng loess. These evidences confirms that the loess in the YRB does not come from the arid areas in the North China. There is a certain similar geochemistry between the Jiujiang and Nanjing loess, indicating that dust materials in both sites are plausible derived from some source. Combined published results with the distribution

characteristics of the aeolian sand hill and the loess in this region, suggesting that the climate of the YRB is generally deteriorated, the winter wind is strengthened, and many regional wind sand-dust deposit systems have been formed under the global background of the decline of the sea level during the last glacial period. Exposed continental shelf and valley floodplain provide abundant dust material for those depositional units. During the formation of the loess in this region, the river and lake floodplain of large and medium-sized rivers have played vital roles. Therefore, those local dust deposits can be called "valley-sourced loess".

#### Acknowledgments

This study is supported by the National Natural Science Foundation of China (No.41262007), the Collaborative Innovation Center for Major Ecological Security Issues of Jiangxi Province and Monitoring Implementation (No.JXS-EW-00), the Innovation Fund Designated for Graduate Students of Jiangxi Normal University(YJS2018069) and the Foundation of Jiangxi Educational Committee (No.8884), the Opening Fund of Key Laboratory of Poyang Lake Wetland and Watershed Research(Jiangxi Normal University), Ministry of Education (PK2018004).

#### References

- An Z (2000) The history and variability of the East Asian paleomonsoon climate. *Quaternary Science Reviews* 19: 171-187. [https://doi.org/10.1016/s0277-3791\(99\)00060-8](https://doi.org/10.1016/s0277-3791(99)00060-8)
- An Z, Kutzbach JE, Prell WL, et al. (2001) Evolution of Asian monsoons and phased uplift of the Himalaya-Tibetan plateau since Late Miocene times. *Nature* 411: 62-66. <https://doi.org/10.1038/35075035>
- Broecker WS, Peng TH (1982) Tracers in the Sea. Eldigio Press, New York. <https://doi.org/10.2307/1309641>
- Bhatia MR, Crook KA W (1986) Trace element characteristics of graywackes and tectonic setting discrimination of sedimentary basins. *Contributions to Mineralogy Petrology* 92: 181-193. <https://doi.org/10.1007/BF00375292>
- Barth MG, McDonough WF, Rudnick RL (2000) Tracking the budget of Nb and Ta in the continental crust. *Chemical Geology* 165: 197-213. [https://doi.org/10.1016/S0009-2541\(99\)00173-4](https://doi.org/10.1016/S0009-2541(99)00173-4)
- Cox R, Lowe DR, Cullers RL (1995) The influence of sediment recycling and basement composition on evolution of mudrock chemistry in the southwestern United States. *Geochimica & Cosmochimica Acta* 59: 2919-2940. [https://doi.org/10.1016/0016-7037\(95\)00185-9](https://doi.org/10.1016/0016-7037(95)00185-9)
- Chen YY, Li XS, Han ZY, et al. (2008) Chemical weathering intensity and element migration feature of the Xiashu loess profile in Zhengjiang, Jiangsu Province. *Journal of Geographical Sciences* 18: 341-352. <https://doi.org/10.1007/s11442-008-0341-9>
- Chen J, Li GJ (2011) Geochemical studies on the source region of Asian dust. *Science China Earth Sciences* 54: 1279-1301. (In Chinese) <https://doi.org/10.1007/s11430-011-4269-z>
- Chen J, Li G, Yang J, et al. (2007) Nd and Sr isotopic characteristics of Chinese deserts: Implications for the provenances of Asian dust. *Geochimica et Cosmochimica Acta* 71: 3904-3914. <https://doi.org/10.1016/j.gca.2007.04.033>
- Ding Z, Liu T, Rutter NW, et al. (1995) Ice-volume forcing of East Asian winter monsoon variations in the past 800,000 years. *Quaternary Research* 44: 149-159. <https://doi.org/10.1006/qres.1995.1059>
- Gallet S, Jahn BM, Torii M. (1996) Geochemical characterization of the Luochuan loess-paleosol sequence, China, and paleoclimatic implications. *Chemical Geology* 133: 67-88. [https://doi.org/10.1016/S0009-2541\(96\)00070-8](https://doi.org/10.1016/S0009-2541(96)00070-8)
- Guan QY, Pan BT, Gao HS, et al. (2008) Geochemical evidence of the Chinese loess provenance during the Late Pleistocene.

- Palaeogeography, Palaeoclimatology, Palaeoecology 270: 53-58. <https://doi.org/10.1016/j.palaeo.2008.08.013>
- García R, Petidomínguez MD, Rucadio MI, et al. (2011) Provenance of loess from the Spanish central region: chemometric interpretation. Geological Magazine 148: 481-491. <https://doi.org/10.1017/s0016756810000889>
- Guo ZT (2017) Loess Plateau attests to the onsets of monsoon and deserts. Scientia Sinica Terra 47: 421-437. (In Chinese) <https://doi.org/10.1360/No72017-00037>
- Hao QZ, Guo ZT, Qiao YS, et al. (2010) Geochemical evidence for the provenance of middle Pleistocene loess deposits in southern China. Quaternary Science Review 29: 3317-3326. <https://doi.org/10.1016/j.quascirev.2010.08.004>
- Hong HL, Wang CW, Zeng KF, et al. (2013) Geochemical constraints on provenance of the mid-Pleistocene red earth sediments in subtropical China. Sedimentary Geology 290: 97-108. <https://doi.org/10.1016/j.sedgeo.2013.03.008>
- Hu XF, Gong AT (1999) A "Yellow Cap" on Quaternary Red Clay in Jiujiang, Jiangxi Province. Pedosphere 9: 311-318.
- Hu YP, Jia YL, Zhang Z, et al. (2013) Sand loess system in the middle reaches of Yangtze River since late Interglacial indicated by Grain Size. Journal of Desert Research 33: 1324-1332. (In Chinese) <https://doi.org/10.7522/j.issn.1000-694X.2013.00137>
- Jia YL, Lai ZP, Zhang JR, et al. (2012) Chronology and provenance of aeolian sediments in the middle reaches of the Yangtze River in China. Quaternary Geochronology 10: 44-49. <https://doi.org/10.1016/j.quageo.2012.01.011>
- Liu TS (1985) Loess and the Environment Beijing: Science Press. pp 1-412. (In Chinese)
- Lai ZP, Zhou J, Xia YF, et al. (2001) Luminescence dating of Xiashu loess in Nanjing. Progress Nature Science 11: 203-207. (In Chinese) <https://doi.org/10.3321/j.issn:1002-008X.2001.02.016>
- Lai ZP, Zhang WG, Chen X, et al. (2010) OSL chronology of loess deposits in East China and its implications for East Asian monsoon history. Quaternary Geochronology 5: 154-158. <https://doi.org/10.1016/j.quageo.2009.02.006>
- Li XG, He JH, Li DS, et al. (1993) The preliminary test of ESR in Xiashu loess dating. Journal of Nanjing Normal University (Natural Science) 3: 86-91. (In Chinese)
- Li XS, Han ZY, Yang DY, et al. (2006) Aeolian-dust deposit to the southwest of the Poyang lake during the last glacial age. Marine Geology & Quaternary Geology 25: 101-108. (In Chinese)
- Li JW, Qiao YS, Wang Y, et al. (2009) Aeolian origin of the red earth formation in Jiujiang city of Jiangxi province, China: evidence from grain size analysis. Journal of Geomechanics 15: 95-104. (In Chinese) <https://doi.org/10.3969/j.issn.1006-6616.2009.01.009>
- Li XS, Han ZY, Lu HY, et al. (2018) Onset of Xiashu loess deposition in southern China by 09 Ma and its implications for regional aridification. Science China Earth Sciences 61: 256-269. <https://doi.org/10.1007/s11430-017-9134-2>
- Li N, Hao QZ, Zhang XJ, et al. (2016) Geochemical evidence for the provenance of loess deposits in the eastern mountains, central China. Quaternary Sciences 36: 332-346. (In Chinese) <https://doi.org/10.11928/j.issn.1001-7410.2016.02.09>
- Li GJ, Li L, Xu SJ, et al. (2017) Dust source of the loess deposits in the eastern China constrained by uranium communition age. Quaternary Sciences 37:1037-1044. (In Chinese) <https://doi.org/10.11928/j.issn.1001-7410.2017.05.11>
- Liu J, Wu XH, Li SQ, et al. (1997) The last glacial stratigraphic sequence, depositional environment and climatic fluctuations from the aeolian sand dune in Hongguang, Pengze, Jiangxi (China). Quaternary Science Reviews 16: 535-546. [https://doi.org/10.1016/S0277-3791\(96\)00074-1](https://doi.org/10.1016/S0277-3791(96)00074-1)
- Liu F, Li GJ, Chen J (2014) U-Pb ages of zircon grains reveal a proximal dust source of the Xiashu loess, Lower Yangtze River region. China Science Bulletin 59: 2391-2395. <https://doi.org/10.1007/s11434-014-0318-2>
- Meng X, Liu L, Balsam W, et al. (2015) Dolomite abundance in Chinese loess deposits: A new proxy of monsoon precipitation intensity. Geophysical Research Letters 42(10): 391-310, 398. <https://doi.org/10.1002/2015GL066681>
- Meng X, Liu L, Wang XT, et al. (2018) Mineralogical evidence of reduced East Asian summer monsoon rainfall on the Chinese loess plateau during the early Pleistocene interglacials. Earth and Planetary Science Letters 486: 61-69. <https://doi.org/10.1016/j.epsl.2017.12.048>
- Meng X, Liu L, Zhao W, et al. (2019) Distant Taklimakan Desert as an important source of aeolian deposits on the Chinese Loess Plateau as evidenced by carbonate minerals. Geophysical Research Letters 46(9): 4854-4862. <https://doi.org/10.1029/2018GL081551>
- Muhs DR, Bettis III EA. (2003) Quaternary loess-paleosol sequences as examples of climate-driven sedimentary extremes. Geological Society of America 370: 53-74. <https://doi.org/10.1130/0-8137-2370-1.53>
- Muhs DR, Bettis EA, Aleinikoff JN, et al. (2008) Origin and paleoclimatic significance of late Quaternary loess in Nebraska: Evidence from stratigraphy, chronology, sedimentology, and geochemistry. Geological Society of America Bulletin 120: 1378-1407. <https://doi.org/10.1130/B26221.1>
- Muhs DR, Bettis III, EA. (2000) Geochemical variations in Peoria Loess of western Iowa indicate paleowinds of midcontinental North America during last glaciation. Quaternary Research 53: 49-61. <https://doi.org/10.1006/qres.1999.2090>
- Muhs DR (2013) The geologic records of dust in the Quaternary. Aeolian Research 9: 3-48. <https://doi.org/10.1016/j.aeolia.2012.08.001>
- Muhs DR, Budahn JR, Skipp GL, et al. (2016) Geochemical evidence for seasonal controls on the transportation of Holocene loess, Matanuska Valley, southern Alaska, USA. Aeolian Research 21: 61-73. <https://doi.org/10.1016/j.aeolia.2016.02.005>
- Muhs DR. (2018) The geochemistry of loess: Asian and North American deposits compared. Journal of Asian Earth Sciences 155:81-115. <https://doi.org/10.1016/j.jseas.2017.10.032>
- Nie J, Stevens T, Rittner M, et al. (2015) Loess Plateau storage of Northeastern Tibetan Plateau-derived Yellow River sediment. Nature Communication 6: 8511. <https://doi.org/10.1038/ncomms9511>
- Peng XM, Jia YL, Hu YP, et al. (2014) The grain-size features and significance of Xiashu loess profile of Furong-Zhouxi in the north of Jiangxi province. Tropical Geography 34: 663-671. (In Chinese)
- Pye K. (1995) The nature, original and accumulation of loess. Quaternary Science Reviews 14: 653-667. [https://doi.org/10.1016/0277-3791\(95\)00047-X](https://doi.org/10.1016/0277-3791(95)00047-X)
- Peng SZ, Hao QZ, Zhang W, et al. (2016) Geochemical and grain-size evidence for the provenance of loess deposits in the Central Shandong Mountains region, northern China. Quaternary Research 85: 290-298. <https://doi.org/10.1016/j.yqres.2016.01.005>
- Qian P, Zheng XM, Chen J, et al. (2018) Tracing the provenance of aeolian loss in the Yangtze River Delta through zircon U-Pb age and geochemical investigations. Journal of Mountain Science 15(4):708-721. <https://doi.org/10.1007/s11629-017-4437-5>
- Qiao YS, Hao QZ, Peng SS, et al. (2011) Geochemical characteristics of the eolian deposits in southern China, and their implications for provenance and weathering intensity. Palaeogeography, Palaeoclimatology, Palaeoecology 308: 513-523. <https://doi.org/10.1016/j.palaeo.2011.06.003>
- Samuel KM, Balz SK, McGowan A (2005) Provenance of long-travelled dust determined with ultra-trace-element composition: A Pilot study with samples from New Zealand glaciers. Earth Surface Processes and Landforms 30: 699-716. <https://doi.org/10.1002/esp.1169>
- Sun JM (2002) Provenance of loess material and formation of loess deposits on the Chinese Loess Plateau. Earth and

- Planetary Science Letters 203: 845-859.  
[https://doi.org/10.1016/S0012-821X\(02\)00921-4](https://doi.org/10.1016/S0012-821X(02)00921-4)
- Sugitani K, Horiuchi Y, Adachi M, et al. (1996) Anomalously low  $\text{Al}_2\text{O}_3/\text{TiO}_2$  values for Archean cherts from the Pilbara Block, Western Australia—possible evidence for extensive chemical weathering on the early earth. *Precambrian Research* 80:49-76. [https://doi.org/10.1016/S0301-9268\(96\)00005-8](https://doi.org/10.1016/S0301-9268(96)00005-8)
- Sheldon ND, Tabor NJ (2009) Quantitative paleoenvironmental and paleoclimatic reconstruction using paleosols. *Earth Science Reviews* 95: 1-52.  
<https://doi.org/10.1016/j.earscirev.2009.03.004>
- Sun Y, Yin Q, Crucifix M, et al. (2019) Diverse manifestations of the mid-Pleistocene climate transition. *Nature Communications* 10: 352.  
<https://doi.org/10.1038/s41467-018-08257-9>
- Tsoar H, Pye K (1987) Dust transport and the question of desert loess formation. *Sedimentology* 34: 139-153.  
<https://doi.org/10.1111/j.1365-3091.1987.tb00566.x>
- Taylor SR, McLennan SM (1985) The continental Crust: Its Composition and Evolution. Blackwell scientific publication, Oxford. pp1-312. <https://doi.org/10.1086/629067>
- Wang XY, Lu HY, Zhang HZ, et al. (2018) Distribution, provenance, and onset of the Xiashu loess in Southeast China with paleoclimatic implications. *Journal of Asian Earth Sciences* 155: 180-187.  
<https://doi.org/10.1016/j.jseaes.2017.11.022>
- Xu YZ (1991) Preliminary study on the time and forming setting of the Xiashu soil, Hefei. *Geology of Anhui* 1: 54-66. (In Chinese)
- Xiong SF, Ding ZL, Liu TS (1999) Comparing of grain size of red soil in northern Jiangxi, loess and desert sand near Beijing. *Chinese Science Bulletin* 44: 1216-1219. (In Chinese)  
<https://doi.org/10.1007/bf03183492>
- Yang DY, Han HY, Zhou LF, et al. (1991) Eolian deposit and environmental change of middle-late Pleistocene in Xuancheng, and provenance south of the lower reaches of the Yangtze River. *Marine Geology & Quaternary Geology* 11: 97-104. (In Chinese)
- Yang DY (1985) Aeolian dunes of late Pleistocene on south bank at the Mid-lower reaches of Yangtze River. *Journal of desert research* 5: 36-43. (In Chinese)
- Yang SY, Wang Z, Guo Y, et al. (2009) Heavy mineral compositions of the Changjiang (Yangtze River) sediments and their provenance-tracing implication. *Journal of Asian Earth Sciences* 35: 56-65.  
<https://doi.org/10.1016/j.jseaes.2008.12.002>
- Yi SW, Li XS, Han ZY, et al. (2018) High resolution luminescence chronology for Xiashu Loess deposits of Southeastern China. *Journal of Asian Earth Sciences* 155: 188-197. <https://doi.org/10.1016/j.jseaes.2017.11.027>
- Yuan S, Maarten AP, Christiaan JB, et al. (2018) Aeolian dust supply from the Yellow River floodplain to the Pleistocene loess deposits of the Mangshan Plateau, central China: Evidence for zircon U-Pb age spectra. *Quaternary Science Reviews* 182: 131-143.  
<https://doi.org/10.1016/j.quascirev.2018.01.001>
- Zhang H, Lu H, Xu X, et al. (2016) Quantitative estimation of the contribution of dust sources to Chinese loess using detrital zircon U-Pb age patterns. *Journal of Geophysical Research-Earth Surface* 121: 2085-2099.  
<https://doi.org/10.1002/2016JF003936>
- Zheng XM, Yu LZ (1991) Aeolian deposit genesis of dare-green hard clay as Holocene basement strata in Shanghai region. *Shanghai Geology* 02: 13-20. (In Chinese)
- Zheng XM, Yan QS (1995) Aeolian loess deposition during the last glacial period in the northern Jiangsu plain of the Yangtze delta and western areas of the yellow sea and the east china sea. *Quaternary Sciences* 3: 258-266. (In Chinese)
- Zhao SL, Yu HJ, Liu JP (1997) Origin, development and evolutionary model of shelf desertization environment in late stage of Upper Pleistocene. *Science in China Series D: Earth Sciences* 40: 207-214. <https://doi.org/10.1007/BF02878380>
- Zhuang JP, Jia YL, Ma CM, et al. (2007) Eolian Deposits in the Middle Reaches of the Yangtze River during late interstadial of the last glacial (40-22KaBP) and its environmental significance. *Acta Sedimentological Sinica* 25: 424-428. (In Chinese)  
<https://doi.org/10.3969/j.issn.1000-0550.2007.03.014>